NANO LETTERS

pubs.acs.org/NanoLett

Transition from Isolated to Collective Modes in Plasmonic Oligomers

Mario Hentschel,[†,‡] Michael Saliba,[†,‡] Ralf Vogelgesang,[‡] Harald Giessen,[†] A. Paul Alivisatos,[§] and Na Liu*[,§]

[†]4. Physikalisches Institut and Research Center Scope, Universität Stuttgart, D-70569 Stuttgart, Germany, [‡]Max-Planck-Institut für Festkörperforschung, Heisenbergstrasse 1, 70569 Stuttgart, Germany, and [§]Department of Chemistry, University of California, Berkeley, and Materials Sciences Division, Lawrence Berkeley National Laboratory, Berkeley, California 94720

ABSTRACT We demonstrate the transition from isolated to collective optical modes in plasmonic oligomers. Specifically, we investigate the resonant behavior of planar plasmonic hexamers and heptamers with gradually decreasing the interparticle gap separation. A pronounced Fano resonance is observed in the plasmonic heptamer for separations smaller than 60 nm. The spectral characteristics change drastically upon removal of the central nanoparticle. Our work paves the road toward complex hierarchical plasmonic oligmers with tailored optical properties.

KEYWORDS Plasmons, coupling, Fano resonances, dark mode, oligomer

The creation of artificial molecules, in which the roles of atoms are played by nanoparticles, is an extremely promising area of research. Just as atoms join together in myriad different combinations and arrangements to form all the substances in the universe, so we can imagine creating a diverse range of new materials by combining together artificial atoms into artificial molecules and solids.[1] While several coupling mechanisms between nanoparticles can be envisioned, the plasmon coupling between metallic nanoparticles is of great current interest. A metal nanoparticle supports localized surface plasmons, which are associated with the collective oscillation of the conductive electrons in the nanoparticle.[2,3] The electromagnetic field surrounding a metallic nanoparticle excited near the plasmon resonance can extend quite some distance away, so that a compelling analogy exists between plasmon resonances of nanoparticle assemblies and wave functions of simple atoms and molecules.[4] The strong interactions of plasmons in nanoparticle assemblies can render possible many useful applications including surface-enhanced spectroscopies, nanoantennas, and biochemical sensors.[5]

In chemistry, molecular symmetry is one important concept to predict and understand the complex electronic states in molecules evolving from the individual atomic orbitals.[6] For example, the beautiful symmetry of benzene allowed for the invention of the Hückel theory,[7] which provides the qualitative basis for unraveling the energy levels of the molecular orbitals in conjugated hydrocarbon molecules. In plasmonics, thus far relatively simple artificial molecules have been developed from metallic nanostructures including dimers,[8−10] trimers,[11] quadrumers,[12] etc.[13] Despite the tremendous progress in the exploration of dimer nanoparticles,[8−10,14] there have been few theoretical studies devoted to investigating the optical properties of multinanoparticle assemblies.[15−17] A comprehensive experimental study is still missing. In this Letter, we present a detailed study on plasmonic oligomers consisting of six (ring-type hexamer) and seven nanoparticles (heptamer), which have the D_{6h} spatial symmetry of the benzene molecule. We show that the near-field interaction between neighboring elements determines the optical response of the plasmonic oligomers. Importantly, we theoretically and experimentally demonstrate the transition from isolated to collective modes when the six satellite nanoparticles approach the center nanoparticle, akin to the formation of molecular orbitals from individual atomic orbitals in molecules.[1] We further demonstrate the possibility to switch on and off a dark Fano resonance[18−20] by the presence or absence of the central nanoparticle without breaking the system symmetry. The resulting Fano resonance is attributed to the hybridization of the plasmons in the central nanoparticle and the ringlike hexamer. The ability to observe and tune the collective resonances in plasmonic nanostructures will allow for the creation of a rich new set of artificial molecules with a wide range of controlled optical properties.

Figure 1 shows the illustrations of the molecular geometries of an H atom, an H_2 molecule, and a benzene molecule as well as their corresponding plasmonic analogues, namely, a gold monomer, a gold dimer, and a gold hexamer. When light interacts with a gold monomer, dipolar plasmons can be excited in the metallic nanoparticle.[3] When a second gold monomer is brought in close proximity, the plasmons in the two nanoparticles mix and hybridize, giving rise to the

* To whom correspondence should be addressed, nliu@lbl.gov.
Received for review: 6/1/2010
Published on Web: 06/29/2010

DOI: 10.1021/nl101938p | *Nano Lett.* **2010,** *10,* 2721–2726

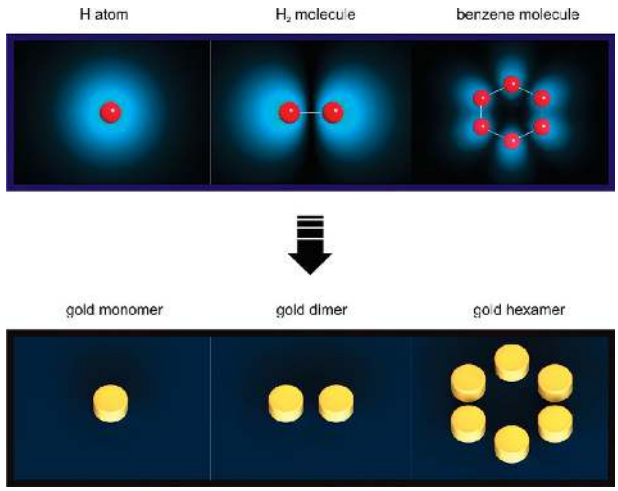

FIGURE 1. (upper row) Illustrations of the molecular geometries of an H atom, an H_2 molecule, and a benzene molecule. (bottom row) Their plasmonic analogues, a gold monomer, a gold dimer, and a gold hexamer. The formation of artificial molecules draws on the compelling analogy to the formation of molecules from simple atoms in chemistry.

formation of antibonding and bonding plasmonic modes.[10] This is in direct analogy to the electron wave functions of two H atoms mixing and hybridizing in order to form molecular orbitals in a H_2 molecule. Furthermore, in analogy to a benzene molecule, the structure of the plasmonic hexamer belongs to the D_{6h} point group, which exhibits a high spatial symmetry. The interaction of light and the gold hexamer can lead to the excitation of collective plasmons in the nanoparticles. In the following, we are going to experimentally study the optical response of the hexamer structure. Particularly, we will demonstrate the remarkable change of its resonant behavior when introducing a central nanoparticle. The optical response of the resulting heptamer structure shows a prominent transition upon gradually reducing the interparticle gap distance.

We have fabricated samples with various geometries including gold monomer, gold hexamer, and a series of gold heptamers with different interparticle gap distances. The structural geometries were defined by electron-beam lithography in a positive resist (PMMA) on a glass substrate. The gold structures were generated by thermal evaporation followed by a lift-off procedure. Each sample has a footprint of 100 μm × 100 μm. Electron micrographs of the fabricated samples were obtained by field-emission scanning electron microscopy (SEM). The top picture in Figure 2 presents an overview SEM image of a typical heptamer structure, demonstrating the high quality of the sample over a large area. The periodicities in both directions are 900 nm. The interparticle gap distance is defined as g, being 20 nm in this heptamer structure. The thickness of the gold nanoparticles is 80 nm. The base diameters of the central nanoparticle and the six satellite nanoparticles are 160 and 150 nm, respectively. The bottom images in Figure 2 present the enlarged views of the sample at a tilting angle of 70°, demonstrating

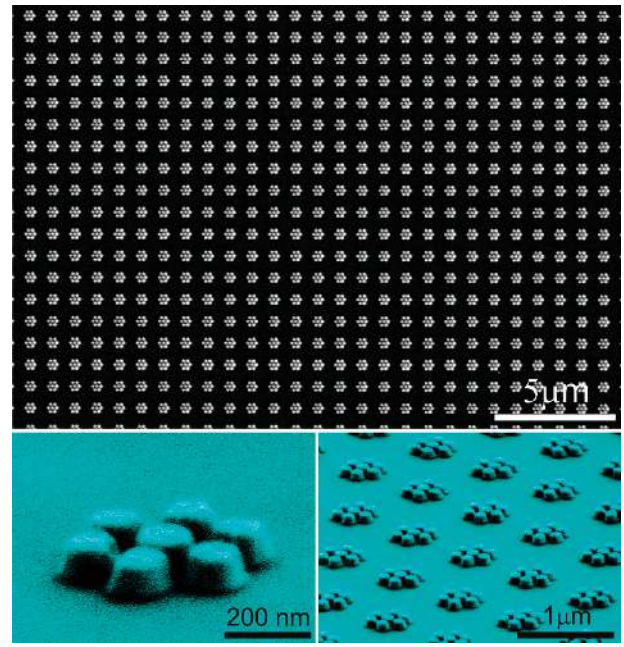

FIGURE 2. SEM images of a typical gold heptamer sample fabricated by electron-beam lithography. (top) A normal view of the sample. The periodicities in both directions are 900 nm. The interparticle gap distance is defined as g, being 20 nm in this heptamer structure. The thickness of the gold nanoparticles is 80 nm. The base diameters of the central nanoparticle and the six satellite nanoparticles are 160 and 150 nm, respectively. (bottom) Enlarged views of the sample at a tilting angle of 70°. The gold nanoparticles have a slight trapezoidal shape resulting from the lift-off procedure.

the homogeneity of the interparticle gap separation. The gold nanoparticles have a slight trapezoidal shape resulting from the lift-off procedure.

In order to investigate the evolution of the coupling behavior, the optical response of a series of nanoparticle oligomers with various interparticle gap distances was evaluated using a Fourier-transform infrared spectrometer, giving extinction (1-transmittance) spectra. The interparticle gap distance g was decreased from 130 to 20 nm. For excitation of the structures, we used normal incident light with linear polarization as shown in Figure 3. The experimental spectra of the samples and their corresponding SEM images are displayed in the same figure. The spectrum of the gold monomer is plotted as a green curve in the bottom row. A single dipolar resonance is observed around 700 nm (the curve is magnified by a factor of 5 for better comparability). Turning toward the heptamer with a large interparticle gap distance (g = 130 nm), the spectrum shows approximately the same behavior as the isolated nanoparticle due to the well-separated nanoparticle configuration. This would correspond in molecular chemistry to the situation of uncoupled atoms before they start to form molecular bonds.[1] As the interparticle gap distance is reduced (g = 60 nm), a second peak starts to form around 800 nm. The two peaks are separated by a pronounced dip. As the interparticle gap distance is further reduced toward g = 20 nm, the spectral features red shift successively. In the ringlike hexamer (g =

DOI: 10.1021/nl101938p | *Nano Lett.* **2010,** *10,* 2721–2726

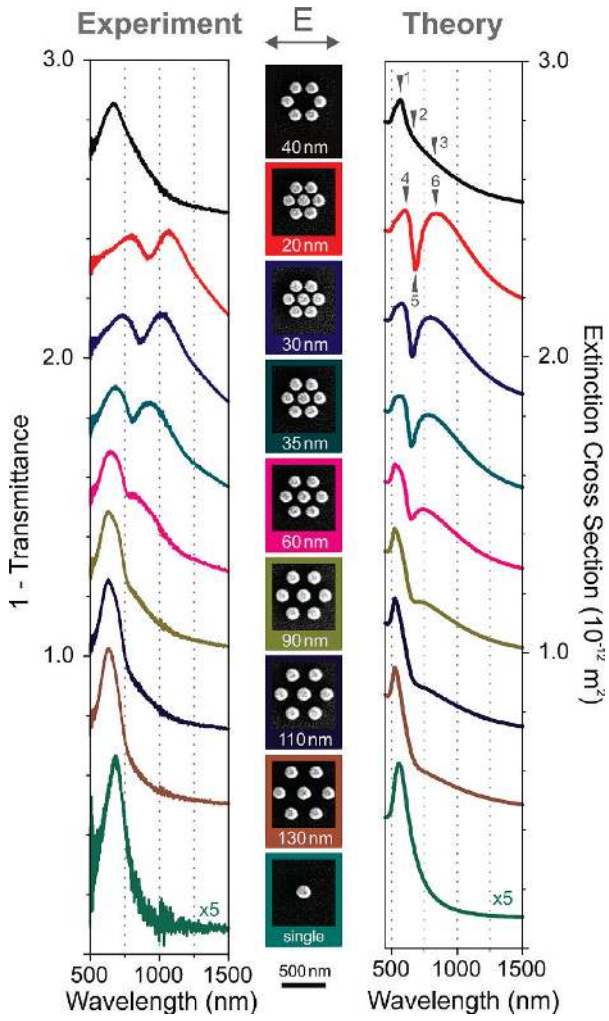

FIGURE 3. Extinction spectra of a gold monomer, a gold hexamer, and gold hepatmers with different interparticle gap separations. Spectra are shifted upward for clarity. (left column) The experimental extinction spectra (1-transmittance). (middle column) SEM images of the corresponding samples with indicated interparticle gap distances. The scale bar dimension is 500 nm. (right column) Simulated extinction cross-section spectra using the multiple multipole method. The gold structures are embedded in air. The difference between the experimental and simulated spectra is due to the presence of the glass substrate in the experiment and it is also partially due to the assumption of a nanosphere shape for the trapezoidal nanoparticles in the simulation. In the gold monomer and hexamer, dipolar plasmon resonances are observed. The transition from isolated to collective modes is clearly visible in the different heptamers when decreasing the interparticle gap distance. Specifically, a pronounced Fano resonance is formed as characterized by the distinct resonance dip when the interparticle gap distance is below 60 nm. The presence or absence of the central nanoparticle can switch on or off the formation of the Fano resonance.

40 nm), which we display for comparison (see the top black spectrum), the shorter-wavelength peak around 700 nm is also present. In contrast to the heptamers, no pronounced dip is visible in the hexamer. We rather observe a long and unstructured tail toward the long wavelength region.

In order to analyze the underlying physics of the observed resonant coupling transition, simulations were performed using a multiple multipole method,[21] which is a semianalytical simulation theory based on Mie scattering. The simulated field distribution is described by a sum of distributed expansions, which are analytical solutions of Maxwell's equations, and the coefficients of the expansions are solved at the boundaries. Currently, we cannot calculate truncated cones or consider the glass substrate within our multiple multipole simulation. In the calculations, we therefore used gold nanospheres with a diameter of 160 nm for the central particle and 150 nm for the six satellite particles. The gold nanostructures were surrounded by air. An experimentally measured dielectric function of gold was utilized in the simulations.[22] Figure 3 presents the simulated extinction spectra for different structures. It is apparent that the experimental results show a good qualitative agreement with the numerical predictions. The overall red shift of the experimental spectra with respect to the simulated spectra is due to the presence of the glass substrate in the experiment. The difference between the experimental and simulated results is also partially due to the assumption of a nanosphere shape for the trapezoidal nanoparticles in the simulation. Nevertheless, all the main spectral features including the distinct resonance dip are clearly predicted.

In order to elucidate the character of the resonances, field distributions at the respective spectral positions are shown in Figure 4. In the hexamer structure, at spectral positions 1, 2, and 3, the currents in the six nanoparticles always oscillate in-phase, manifesting the excitation of the collective dipolar plasmon resonance in the ringlike hexamer. In the heptamer structure, when a central nanoparticle is brought into close proximity of the six satellite nanoparticles, the dipolar plasmon of the central nanoparticle hybridizes with the hexamer dipolar plasmon, giving rise to the formation of a bright superradiant collective mode and a dark subradiant collective mode.[23,24] For the superradiant mode, the oscillating plasmons in the seven nanoparticles are in-phase (see field distributions at spectral positions 1 and 3), exhibiting significant mode broadening due to radiative damping.[25,26] It is worth mentioning that the peak position of the superradiant mode cannot be exactly determined from the spectrum due to the presence of the resonance dip. Nevertheless, the resonant behavior at positions 1 and 3 is a good indication for the superradiant mode. For the subradiant mode, the net sum of the plasmon polarizations of the six satellite nanoparticles oscillates oppositely with respect to the plasmon polarization in the central nanoparticle (see field distribution at spectral position 2). The unique symmetry of the heptamer allows for similar yet opposite dipole moments of the central nanoparticle and the ringlike hexamer, thus leading to a narrow mode.[25,26] The formation of the distinct dip in the spectrum is due to the destructive interference between the narrow subradiant mode and the broad superradiant mode, which is called a Fano resonance.[19,20] Such a Fano resonance is only observable in the presence

DOI: 10.1021/nl101938p | *Nano Lett.* **2010,** *10,* 2721–2726

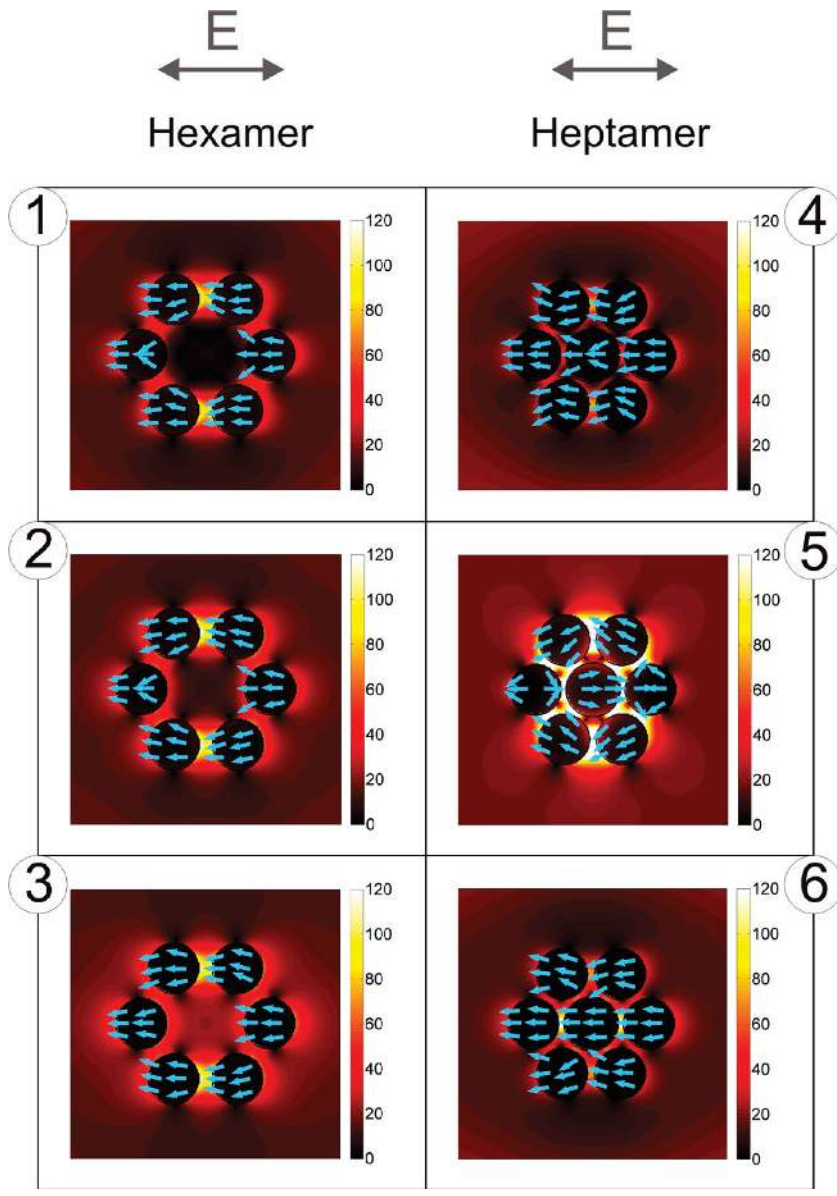

FIGURE 4. Simulated field distributions for the gold hexamer and heptamer at the respective spectral positions (as indicated by the arrows in Figure 3) using the multiple multipole method. It is notable that at spectral position 5 in the heptamer, similar yet opposite oscillating plasmons are excited in the central nanoparticle and the ringlike hexamer, thus leading to a subradiant mode. The destructive interference between the subradiant mode and the broad superradiant mode results in the Fano resonance. In the absence of the central nanoparticle, the nanoparticles in the hexamer always oscillate in phase, leading to a collective dipolar mode.

of the central nanoparticle. In other words, the central nanoparticle can be utilized to switch on and off the Fano resonance.

In the weak coupling region at $g \geq 110$ nm, the nanoparticles are relatively well separated and the single resonance does not show an obvious spectral shift when decreasing g. At 60 nm $\leq g <$ 110 nm, the coupling between the nanoparticles becomes stronger and the signature of the Fano resonance comes into existence. The dipolar plasmons of the central nanoparticle start to hybridize with the plasmons of the ringlike hexamer, leading to the formation of the subradiant and superradiant modes. Nevertheless, in this intermediate coupling region, the superradiant mode, which is at a shorter wavelength compared to the subradiant mode, does not have a broad enough line width to substantially overlap with the narrow subradiant mode. As a result, the Fano resonance manifests itself as an asymmetric kink at the right shoulder of the superradiant mode (for example see $g = 90$ nm). At 20 nm $\leq g <$ 60 nm, the nanoparticles in the heptamer experience strong coupling and form collective plasmonic modes. Due to the strong in-phase plasmon oscillation in the seven nanopaticles, the superradiant mode undergoes a significant broadening and a

DOI: 10.1021/nl101938p | *Nano Lett.* **2010,** *10,* 2721–2726

spectral red shift, while the subradiant mode remains narrow. Consequently, the superradiant mode has a broad enough spectral profile to overlap with the subradiant mode. The conditions of the destructive interference effects are thus sufficiently fulfilled,[24,25] giving rise to a more pronounced Fano resonance (for example see $g =$ 20 nm). In essence, the interparticle gap distance substantially dictates the transition from isolated to collective modes and plays a crucial role for the formation of the Fano resonance in the plasmonic heptamer. It is noteworthy that the line width of the Fano resonance is essentially determined by the intrinsic damping in the metal and the net dipole moment of the subradiant mode.[24,25] Reducing losses in the metal and optimizing the structural parameters to obtain a reduced net dipole moment are the keys to achieve darker Fano resonances all the way toward electromagnetically induced transparency (EIT)-like resonances.[25−29] In plasmonics, Fano and EIT-like resonances are of special interest due to their narrow line width and their sensitive spectral response on the dielectric permittivity of the surrounding environment. These characteristics put our plasmonic oligomer forward as a good platform for achieving plasmonic sensors with a high figure of merit and an extremely small mode volume.[5,26]

In this Letter, we theoretically and experimentally studied the transition from isolated to collective modes in plasmonic oligomers. The interparticle gap distance plays a key role for the formation of collective modes. We have shown how the plasmon hybridization method can be applied to analyze the optical properties of plasmonic oligomers. The interference between a subradiant mode and a superradiant mode leads to a pronounced Fano resonance, which is governed by the presence of the central nanoparticle in the plasmonic heptamer. The experiment agrees very well with our simulation using the multiple multipole method. We have demonstrated that experimental observation of distinct spectral features is possible in high-quality nanolithographic planar ensemble structures. So far, bottom-up synthesis methods[5] have yielded floppy assemblies, so that it has not been possible to fix the interparticle gap distance in such a precisely controlled fashion, therefore preventing the observation of a transition to collective behavior in plasmonic oligomers.

Molecular chemistry offers a framework to draw inspiration from in the design of artificial molecules using plasmonic oligomers. The well-understood molecular models in chemistry can help nanoscientists to draw on correct intuition from molecular orbital theory to predict the optical response of complex plasmonic oligomers. The bridging of these two disciplines will help in the discovery of numerous useful electromagnetic analogues of chemical molecules in plasmonics. We envision for the future plasmonic oligomers of different hierarchies, including three-dimensional ones, oligomers with defects or extremely high symmetry, oligomers that show aromatization effects,[6] and oligomers functionalized with other materials, such as quantum emitters. The lithographically patterned artificial molecules shown here provide a useful benchmark for bottom-up methods of artificial molecule creation such as DNA scaffolding.[30−32]

Acknowledgment. We thank T. Weiss, P. Braun, and M. Dressel for useful discussions and comments. We acknowledge S. Hein for his material visualizations. M. Hentschel, M. Saliba, R. Vogelgesang, and H. Giessen were financially supported by Deutsche Forschungsgemeinschaft (SPP1391, FOR73, and FOR557), by BMBF (13N9048 and 13N10146), and by BW-Stiftung. N. Liu and A. P. Alivisatos were supported by the Director, Office of Science, Office of Basic Energy Sciences, of the United States Department of Energy under Contract DE-AC02-05CH11231.

REFERENCES AND NOTES

(1) Haken, H.; Wolf, H. C. In *Molecular physics and elements of quantum chemistry*; Springer: Berlin, **2003**.
(2) Barnes, W. L.; Dereux, A.; Ebbesen, T. W. *Nature* **2003**, *424* (6950), 824–830.
(3) Maier, S. In *Plasmonics: fundamentals and applications*; Springer: Berlin, 2007.
(4) Prodan, E.; Radloff, C.; Halas, N. J.; Nordlander, P. *Science* **2003**, *302* (5644), 419–422.
(5) Lal, S.; Link, S.; Halas, N. J. *Nat. Photonics* **2007**, *1*, 641–648.
(6) Carter, R. L. In *Molecular symmetry and group theory*; John Wiley & Sons: New York, 1998.
(7) Hückel, E. *Z. Phys. A* **1931**, *70*, 204–286.
(8) Brown, L. V.; Sobhani, H.; Lassiter, J. B.; Nordlander, P.; Halas, N. J. *Acs Nano* **2010**, *4* (2), 819–832.
(9) Sonnichsen, C.; Reinhard, B. M.; Liphardt, J.; Alivisatos, A. P. *Nat. Biotechnol.* **2005**, *23* (6), 741–745.
(10) Nordlander, P.; Oubre, C.; Prodan, E.; Li, K.; Stockman, M. I. *Nano Lett.* **2004**, *4* (5), 899–903.
(11) Brandl, D. W.; Mirin, N. A.; Nordlander, P. *J. Phys. Chem. B* **2006**, *110* (25), 12302–12310.
(12) Urzhumov, Y. A.; Shvets, G.; Fan, J.; Capasso, F.; Brandl, D.; Nordlander, P. *Opt. Express* **2007**, *15*, 14129–14145.
(13) Jun, Y. W.; Sheikholeslami, S.; Hostetter, D. R.; Tajon, C.; Craik, C. S.; Alivisatos, A. P. *Proc. Natl. Acad. Sci. U.S.A.* **2009**, *106* (42), 17735–17740.
(14) Yang, S. C.; Kobori, H.; He, C. L.; Lin, M. H.; Chen, H. Y.; Li, C. C.; Kanehara, M.; Teranishi, T.; Gwo, S. *Nano Lett.* **2010**, *10* (2), 632–637.
(15) Mirin, N. A.; Bao, K.; Nordlander, P. *J. Phys. Chem. A* **2009**, *113* (16), 4028–4034.
(16) Gomez, D. E.; Vernon, K. C.; Davis, T. J. *Phys. Rev. B* **2010**, *81*, No. 075414.
(17) Le, F.; Brandl, D. W.; Urzhumov, Y. A.; Wang, H.; Kundu, J.; Halas, N. J.; Aizpurua, J.; Nordlander, P. *ACS Nano* **2008**, *2* (4), 707–718.
(18) Fan, J. A.; Wu, C. H.; Bao, K.; Bao, J. M.; Bardhan, R.; Halas, N. J.; Manoharan, V. N.; Nordlander, P.; Shvets, G.; Capasso, F. *Science* **2010**, *328* (5982), 1135–1138.
(19) Verellen, N.; Sonnefraud, Y.; Sobhani, H.; Hao, F.; Moshchalkov, V. V.; Van Dorpe, P.; Nordlander, P.; Maier, S. A. *Nano Lett.* **2009**, *9* (4), 1663–1667.
(20) Sonnefraud, Y.; Verellen, N.; Sobhani, H.; Vandenbosch, G. A. E.; Moshchalkov, V. V.; Van Dorpe, P.; Nordlander, P.; Maier, S. A. *ACS Nano* **2010**, *4* (3), 1664–1670.
(21) Hafner, C. *Phys. Status Solidi B* **2007**, *244* (10), 3435–3447, The platform "OpenMaX" is available at http://openmax.ethz.ch/.
(22) Johnson, P. B.; Christy, R. W. *Phys. Rev. B* **1972**, *6* (12), 4370–4379.

DOI: 10.1021/nl101938p | *Nano Lett.* **2010,** *10,* 2721–2726

(23) Christ, A.; Zentgraf, T.; Tikhodeev, S. G.; Gippius, N. A.; Kuhl, J.; Giessen, H. *Phys. Rev. B* **2006**, *74* (15), 155435−1–8.
(24) Christ, A.; Martin, O. J. F.; Ekinci, Y.; Gippius, N. A.; Tikhodeev, S. G. *Nano Lett.* **2008**, *8* (8), 2171–2175.
(25) Liu, N.; Langguth, L.; Weiss, T.; Kastel, J.; Fleischhauer, M.; Pfau, T.; Giessen, H. *Nat. Mater.* **2009**, *8* (9), 758–762.
(26) Liu, N.; Weiss, T.; Mesch, M.; Langguth, L.; Eigenthaler, U.; Hirscher, M.; Sonnichsen, C.; Giessen, H. *Nano Lett.* **2010**, *10* (4), 1103–1107.
(27) Zhang, S.; Genov, D. A.; Wang, Y.; Liu, M.; Zhang, X. *Phys. Rev. Lett.* **2008**, *101* (4).
(28) Papasimakis, N.; Fedotov, V. A.; Zheludev, N. I.; Prosvirnin, S. L. *Phys. Rev. Lett.* **2008**, 253903.
(29) Tassin, P.; Zhang, L.; Koschny, T.; Economou, E. N.; Soukoulis, C. M. *Phys. Rev. Lett.* **2009**; No. 053901.
(30) Sharma, J.; Chhabra, R.; Cheng, A.; Brownell, J.; Liu, Y.; Yan, H. *Science* **2009**, *323* (5910), 112–116.
(31) Mastroianni, A. J.; Claridge, S. A.; Alivisatos, A. P. *J. Am. Chem. Soc.* **2009**, *131*, 8455–8459.
(32) Park, S. Y.; Lytton-Jean, A. K. R.; Lee, B.; Weigand, S.; Schatz, G. C.; Mirkin, C. A. *Nature* **2008**, *451* (7178), 553–556.

DOI: 10.1021/nl101938p | *Nano Lett.* **2010,** *10,* 2721--2726